Mechanical properties and weld characteristics of friction stir welding of thermoplastics using heat-assisted tool.

SHAH, F., YOUNAS, M., KHAN, M. KHAN, A., KHAN, Z. and KHAN, N.

2023

Mechanical properties and weld characteristics of Friction Stir Welding of thermoplastics using heat-assisted tool

Farooq Shah[1], Muhammad Younas[2*], Mushtaq Khan[3], Ashfaq Khan[2], Zarak Khan[1] and Nawar Khan[4]

[1]Department of Mechanical Engineering, HITEC University Taxila, Pakistan

[2*]School of Engineering, Robert Gordon University Aberdeen United Kingdom

[3]Mechanical Engineering Department, Prince Muhammad Bin Fahad University, Al Khobar 31952, Saudi Arabia

[4]Riphah International University, Al Mizan Campus, Rawalpindi, Pakistan

*Corresponding Author:

Dr Muhammad Younas

m.younas@rgu.ac.uk

Mechanical properties and weld characteristics of Friction Stir Welding of thermoplastics using heat-assisted tool

Abstract

Friction Stir Welding (FSW) is a welding technique in which a non-consumable rotating tool with a profiled pin is pressed on the adjoining surfaces and transverse along the welding direction to produce a weld trail. The technique was first applied to metals and alloys; lately, its use has also been extended to thermoplastic polymers. In this work, FSW of HDPE thermoplastic polymer has been investigated and effort is made to achieve welds properties comparable to the base material. FSW of thermoplastics is different from metals because of their different nature and thermal conductivity. Conventional FSW techniques are not effective in its current form and inhibit many challenges to welding of HDPE. To address these problems, a specialized heat-assisted welding tool was developed, and mounted on CNC machine to carry out extensive welding investigations. Statistical techniques were used to investigate effect of temperature, rotational and transverse speed on the weld characteristics. It was revealed that temperature is the most significant factor followed by rotational and traversing speeds. In general, a higher temperature in combination with lower transverse speeds produced the most desirable results. In terms of ultimate tensile strength (UTS), weld joint efficiency of 98 % of the base material was achieved through optimization of process parameters. Ultimate tensile strength of 23 MPA and combined weld efficiency of 66 % was achieved which is closely comparable to the base material. This work is a leap forward towards understanding FSW of a vast range of the thermoplastic.

Keywords: Friction Stir Welding, thermoplastics, heat-assisted tool, Weld efficiency, CNC machine

1 Introduction

Friction Stir Welding is a promising technique which has been developed by The Welding Institute (TWI) England in 1991 and was first demonstrated on aluminium and its alloys [1]. FSW, in its core form, is a solid-state joining process in which a rotating non-consumable tool, consisting of a pin and shoulder, is plunged into the abutting sides of plates or sheets to be welded and moved along the joint line as depicted in Fig. 1.

FSW method offers many advantages over other existing joining techniques [1], such as: The process can be automated and is suited for robot use. The process retains excellent mechanical properties in fatigue, tensile, and bend tests. It is environment friendly because arcs, fumes, and gas shielding are not used. There is no need of using any filler material. It can weld difficult to weld and dissimilar materials. There is no need for post-processing activities like grinding, brushing, polishing.

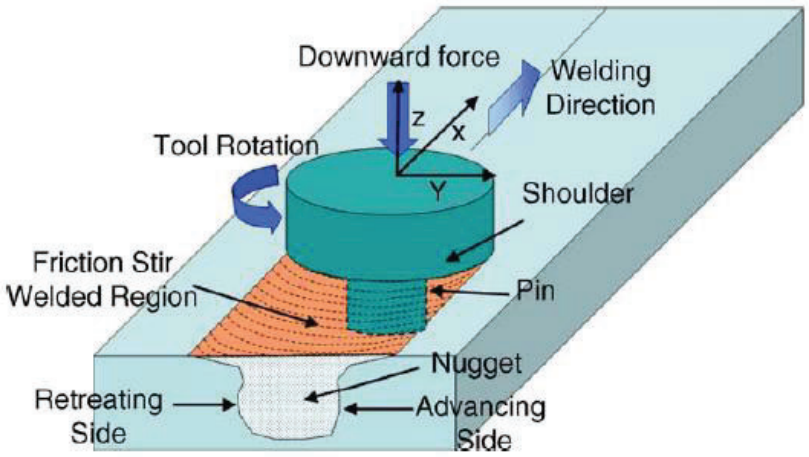

Fig. 1 Friction Stir Welding process [2]

At first, FSW was applied on metal alloys that were difficult to weld with traditional techniques especially the highly alloyed aluminium alloys of series 2XXX and 7XXX. Later on the applicability of the process on thermoplastic materials has also been demonstrated [3]. It has been concluded that the welding process can compete with the established plastic joining techniques with great promise [4]. But the applicability of this technique, in its conventional form, to plastics has resulted in limited success because of the thermal and viscoelastic properties of plastics [5].

Out of the three polymeric materials - thermoplastics, thermosets, and elastomers - only thermoplastics are the weldable polymers because they can be reshaped after heating them below their degradation temperature. The welding parameters, in FSW of thermoplastics, reported in literature are tool rotational and welding speeds, weld temperature, tool profile, length, diameter, and tilt angle, workpiece thickness, dwell time and plunge depth [1]. Selection of proper

parameters and their optimization is crucial for finding significant factors towards the weld quality. The thermoplastic polymers reported in literature are: High Density Polyethylene (HDPE) [6], [7], [8], [9], [10], [11], [12], [13], Medium Density Polyethylene (MDPE) [14], [15], Ultra High Molecular Weight Polyethylene (UHM-PE) [16], Polypropylene (PP) [17], [18], [19], [20], Acrylonitrile butadiene styrene (ABS) [21], [22], [23], [24], Nylon-6 [25], Poly (methyl methacrylate) (PMMA) [5], Polyethylene terephthalate glycol (PETG) [19].

Heat-assisted FSW on HDPE has proved to be a superior technique over the conventional FSW technique as weld efficiencies of 96% [26], 98% [27], and even 104% [10] have been reported in literature for the workpiece thicknesses of 10 mm, 15 mm, 5 mm respectively. Welding on workpiece thicknesses less than 5 mm poses the additional challenges of outpouring and sticking to the shoulder of the tool. No work has been reported yet on welding of workpieces having thickness less than 5 mm hence workpiece thickness of 3 mm is used in this work.

The tooling material used in conventional FSW tools are mostly different grades of steel [1] which doesn't wear out easily while the tooling materials used in Static-shoe or heat-assisted FSW are different grades of Steel [21], [28], [29], [24], [10], Aluminium [9], [30], and Polycarbonate, Teflon, Wood, and Brass [31]. The tooling material used in this work is a low-grade copper for improving heat conductivity in the weld region.

Different Welding tool pin and shoulder designs have been proposed for polymers with the aim of getting quality welds having high joint efficiency, less welding defects, and good surface finish [32], [33]. Kazem et al. concluded that pin of cylindrical geometry is preferred in comparison with conical one [8]. Panneerselvan and Lenin found out in their work of tool forces investigation that threaded pin profile produces the least amount of linear forces on the tool in comparison with triangular, square, grooved with square, taper, and straight pins.

Several attempts have been made to apply conventional FSW tools on polymers but they resulted in low quality welds and though strength efficiency of 86.2% has been reported [7], it still has limited scope while applying on variety of polymeric materials. Scialpi [34] has pointed out the problems related to the FSW conventional tools which are: outpouring of molten material from weld line, low welding speeds, irregular mixing of weld material at weld line, and poor crown surface finish. Hence to address these problems heat-assisted and stationary shoulder techniques have been applied. Hot Shoe and Stationary shoulder approaches are employed for improving joint

strength and minimizing welding defects, but they have an intrinsic shortcoming that they can only be operated in straight lines and requires complex fixture. Aydin [16] has also used an approach of supplying external heat through heating workpieces. In-situ heating has proved to be a good approach towards minimizing common weld defects [21]. Vijendra and Sharma have introduced an in-situ heating technique using induction heating which resulted in 104.32% joint efficiency [10].

This experimental study introduces a novel Heat-assisted FSW tool in which heat is supplied by an internal heater which, in turn, is controlled through PID temperature control mechanism for maintaining uniform heat throughout the welding process. The aim of this study is to assess the efficiency of the friction welding process using a specially designed heat-assisted tool by analyzing different aspects of the weld i.e., joint strength, surface finish, fracturing behaviour, and weld defects. The processing parameters employed in this work are tool rotational speed, tool traversing speed, and weld temperature.

2 Experimental details

The heat-assisted FSW tool used in this work consists of a high speed slip-ring which has the capability of establishing and maintaining electrical connection from a rotating to non-rotating structure over high speeds (up to 5000 rpm) and high current values (up to 5A) along with transmission of electrical signals for communication. The rotating component of slip-ring was mounted on a carbon steel supportive structure to give electrical connection to the heater and thermocouple placed inside the tool's heat-conductive part. The welding tool (Fig. 2 and Fig. 3) was then mounted on CNC milling head and allowed to move during welding along its movements as shown in Figure-4. Electrical connection is thus established an outside stationary structure to the inside rotary heater which in turn is controlled from the signals generated by the thermocouple mounted on tool shoulder.

The thermocouple senses temperature at the tip of the tool and gives feedback signal via slip-ring connection to the outside PID temperature controller. Once the input parameters are set, the two weld-ready pieces are held tightly end to end such that no gap is present between them. After setting a particular temperature value, the heater is turned on and off continuously according

to PID temperature control algorithm. Once the desired temperature value is established, the rotating tool is plunged into the sheets and traversed along the weld line according to the set G&M codes of CNC milling machine. The weld is thus made at the end of the weld line and tool is retracted back and heater turned off.

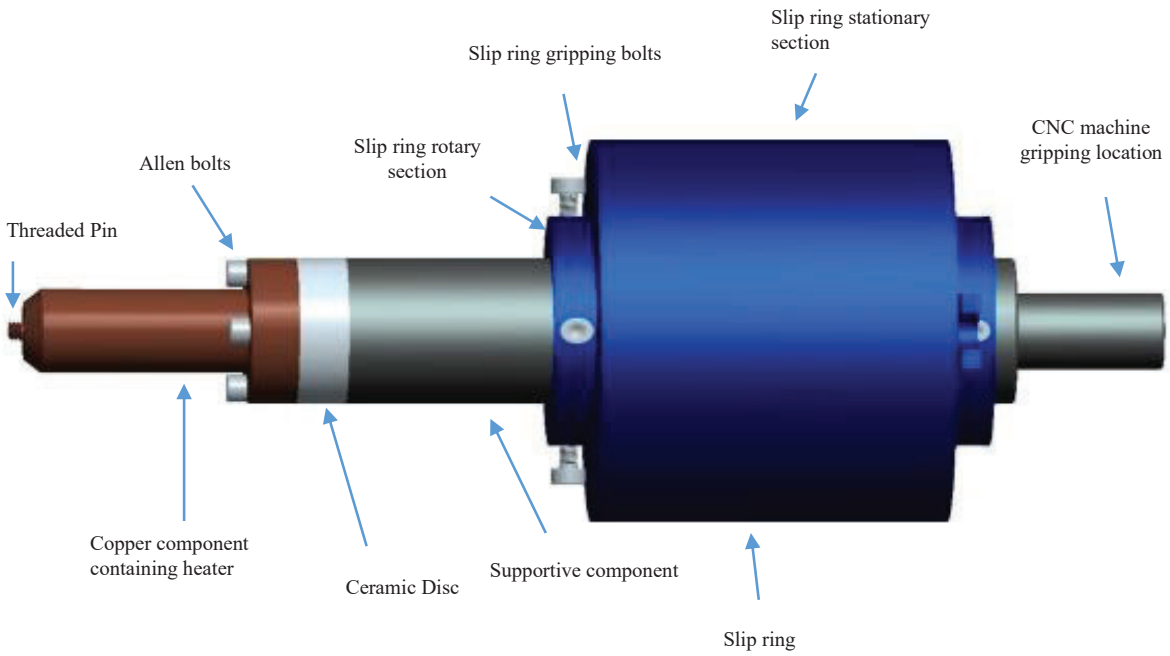

Fig. 2. 3D view of the assembled welding tool

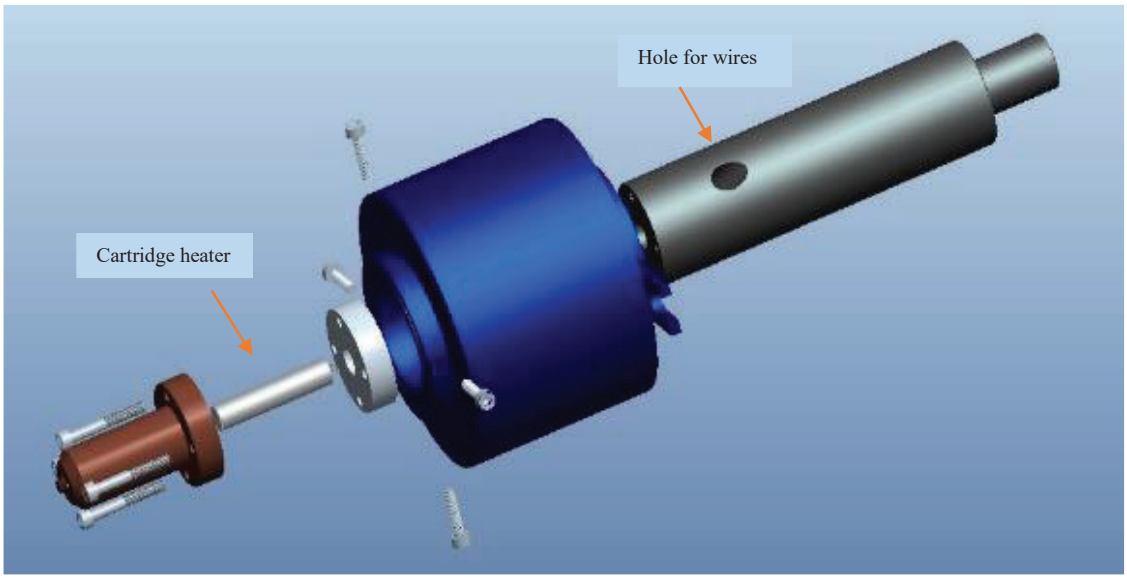

Fig. 3. Exploded view of welding tool

The cylindrical pin helps in uniform stirring of the weld material along with uniform heat flow while the shoulder helps in containing the weld material inside the weld nugget. Temperature is maintained at constant level throughout the welding according to the set instruction by LabVIEW program as shown in Fig. 3.

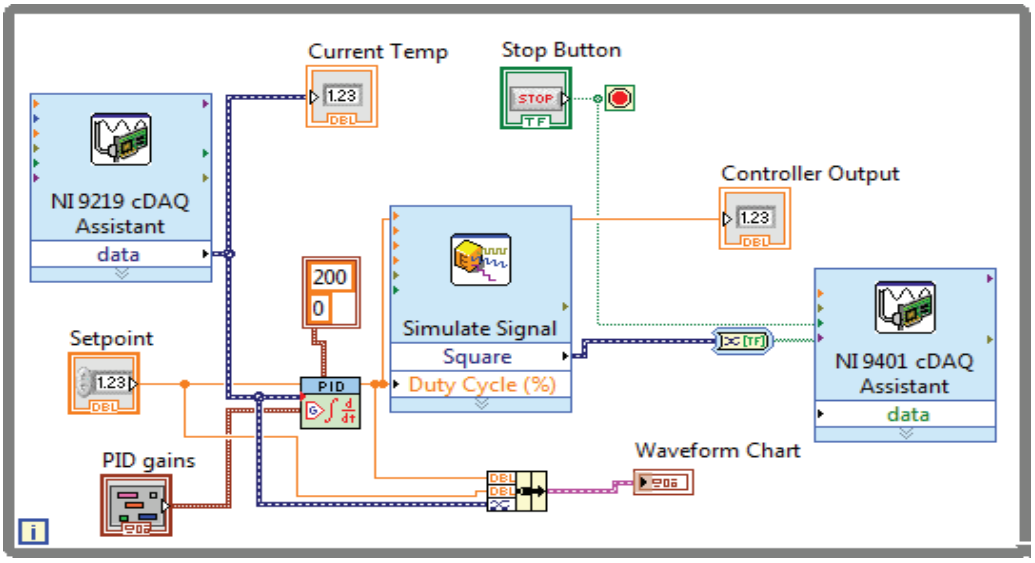

Fig. 3. LabVIEW PID temperature control program

A workpiece cut from 11 mm thick commercial High-Density Polyethylene (HDPE) sheet was used in the welding whose base properties are shown in Table 1. The calculated strength of the base material was 23.5 MPa. Its thickness was reduced to 3 mm on one side on which welding was intended. The thickness was reduced for 38 mm width out of 60 mm. The length of the piece was set at 150 mm. Two such pieces were then placed end to end for butt joining such that its reduced thickness sides were placed next to each other without any gaps in between in a simple fixture on a backing plate inside a vertical CNC milling machine as shown in Fig. 4. The welding tool tip used was made of copper to promote heat flow in the weld line. Its shoulder had a diameter of 15 mm while its cylindrical pin diameter was 5 mm and length 3 mm with M5 threads on it. The pin was right-hand threaded hence the rotation of the pin was set anti-clockwise to promote the downward flow of welded material [10], [21]. After the welding process, the welds were allowed to cool for 10 minutes while still attached to the fixture [26].

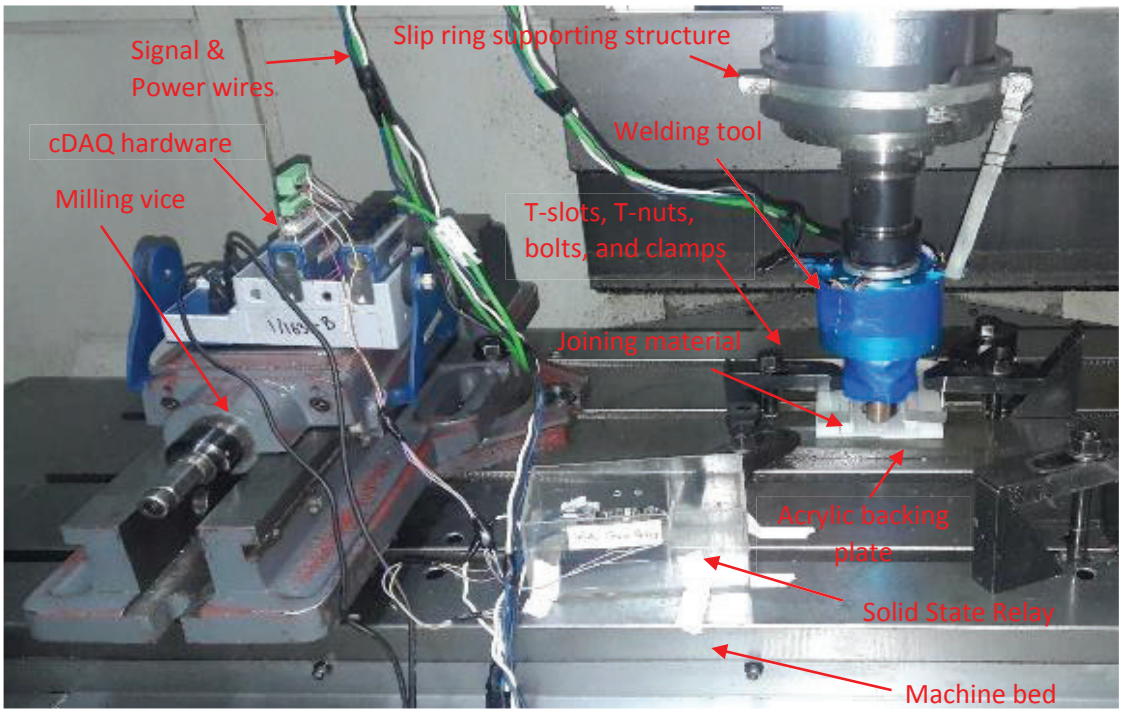

Fig. 4. Welding tool setup inside vertical CNC milling machine

Table-1: Base properties of HDPE

Density (g/cm^3)	**Tensile strength (MPa)**	**Elongation at break (%)**	**Melting temperature range (°C)**
0.96	22-25	600-10000	126-130

The input parameters were chosen through pilot experiments and as result three three-level factors i.e., tool rotational speeds, tool traversing speeds, and weld temperatures were selected as the input processing parameters. An L9 (3^3) orthogonal array was selected from Taguchi designs for experimentation. The factors and its levels are shown in Table 2 while the factors with different levels combination according to Taguchi L9 design is shown in Table 3. The S/N ratios and main effects were used to determine the significant factors and the relationship between the input parameters and the response variable. Macroscopic surface finish and weld defects were also analyzed to determine the best input factors combination.

Table-2: FSW process parameters and levels

Symbol	Welding parameter	Unit	Level 1	Level 2	Level 3
A	Weld temperature	(°C)	120	135	150
B	Tool rotational speed	(rpm)	400	800	1200
C	Tool traversing speed	(mm/min)	8	12	16

Table-3: Experimental layout using an L9 orthogonal array

Experimental run	FSW process parameters		
	A	B	C
	Temperature (°C)	Tool rotational speed (rpm)	Tool traversing Speed (mm/min)
1	120	400	8
2	120	800	12
3	120	1200	16
4	140	400	12
5	140	800	16
6	140	1200	8
7	150	400	16
8	150	800	8
9	150	1200	12

In the conventional FSW processing of polymers, the main purpose of the axial forces is to generate heating through friction which results in the softening of the material. Su et al. [35] stated that the generated frictional heat is proportional to the applied force during welding. However, increase in the axial force does not necessarily result in increasing weld strength as it leads to the squeezing out of the material [23].

In this study, the weld temperature was primarily achieved with a heated tool, resulting in softening of the material. Thus, the study was unique because it did not require an enormous amount of axial force. Almost all of the process parameters relate directly or indirectly to the heat generation and the most important parameter in this setup is the (i) heat input to the joint and (ii) the time for which the heat is supplied.

Therefore, in this study, the parameters such as rotation speed, transverse speed and tool temperature have been varied to identify suitable selection of process parameters for better weld quality. Only a sufficient contact was needed between the tool and the joint material to contain the

material in the weld bead; which has been observed during the experimentation. By employing this technique, it has been shown that the weld defects are reduced and strength of about 96% of the base material has been achieved.

For mechanical tests three tensile specimens were cut in perpendicular direction to the weld from each experimental run according to the ASTM: D638 type-5 standard. Samples were cut from the middle of the welded plates to eliminate the start and end effects of the welding process [20]. Tensile tests were performed on SHIMADZU AG-X Plus table-top model which had a maximum loading capacity of 20 kN. The cross-head speed was kept constant at 10 mm/minute for all samples at room temperature. For each experimental run, tensile test was carried out three times and the average value was calculated from it.

3. Results and Analysis

Surface finish observations and tensile tests of the welded regions were performed in order to assess the weld quality of the joint. Surface finish observations revealed welding defects in certain locations, orientations, and sizes. The tensile tests of the specimens from the joint region for ultimate tensile strength showed how much mechanically strong welds had been made while the percent elongation at break showed how much of the original material plasticity had been retained by the proposed process and the tool developed. The defects and tensile properties showed the effectiveness of the proposed process and tool.

3.1 Material flow and nature of defects:

The surface finish observations and features of the welded joints are shown for each experimental run. They give an indication of how good a welding joint is made. From the Taguchi L9 array, the nine joints welded were of different surface finishes and strengths as shown in Figures 5-13 and Table 4.

Table-4: Ultimate tensile strength & Percent-elongation-at-break of joints

Exp.	Temp. (°C)	Tool rotation (rpm)	Traverse Speed (mm/min)	UTS (MPa)	Elongation-at-Break (%)

1	120	400	8	20	102.7
2	120	800	12	12	17.6
3	120	1200	16	7.8	16.3
4	135	400	12	13.4	108.4
5	135	800	16	22.6	136.6
6	135	1200	8	19.9	85.8
7	150	400	16	23	234.8
8	150	800	8	18.8	98.5
9	150	1200	12	22.6	160
Base material	-	-	-	**23.5**	**692.7**

Joint-1 had cavity defects and flow lines (Fig. 5). Joint-2 had kissing bonds and flow lines (Fig. 6). Joit-3 also had kissing bonds and poor coalescence at the base of the joint (Fig. 7). Joint-4 showed flash to one side of joint and lack-of-fill defect to the other side (Fig. 8). Joint-5 to joint-9 had no obvious defects (Fig. 9 to Fig. 13). Each welded joint had a very specific surface finish and surface texture.

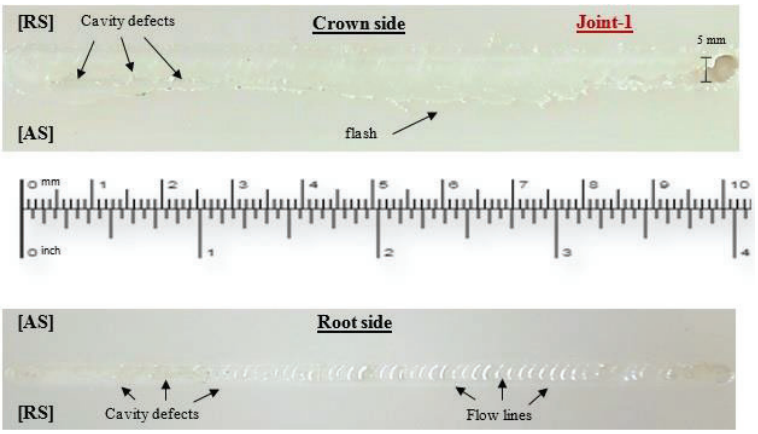

Fig. 5. Joint-1 material flow, surface finish, and surface defects

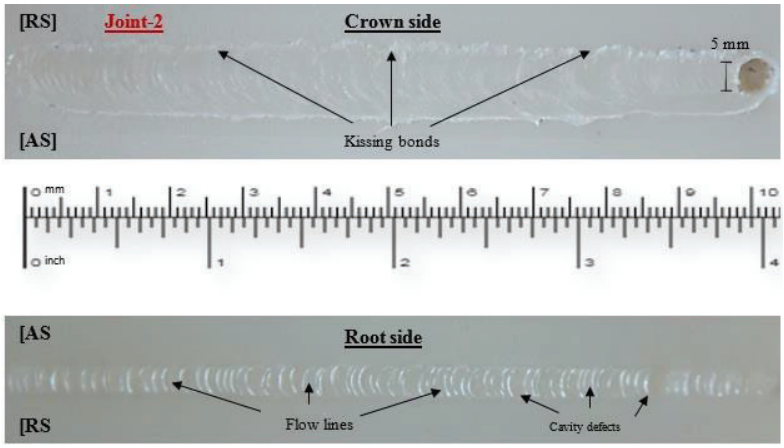

Fig. 6. Joint-2 material flow, surface finish, and surface defects

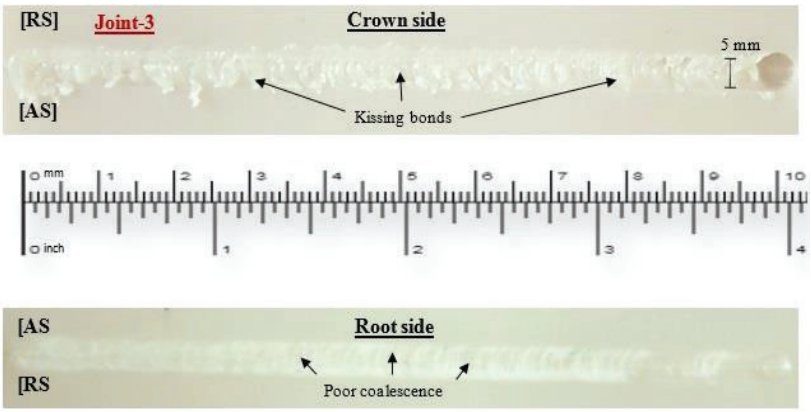

Fig. 7. Joint-3 material flow, surface finish, and surface defects

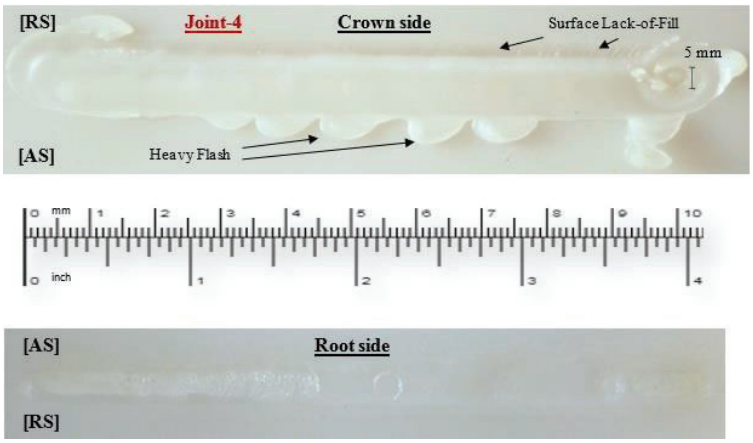

Fig. 8. Joint-4 material flow, surface finish, and surface defects

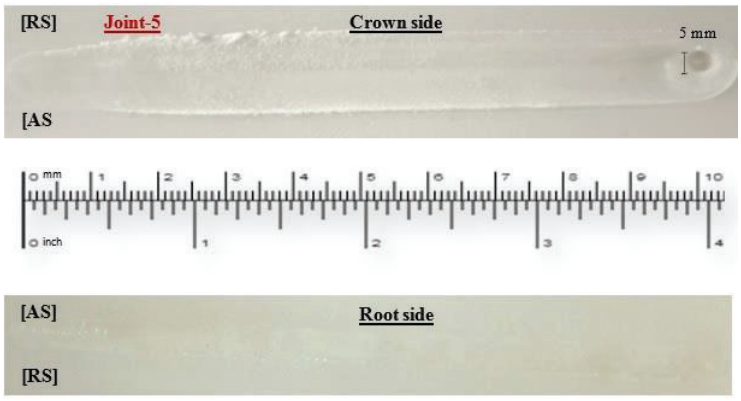

Fig. 9. Joint-5 material flow, surface finish, and surface defects

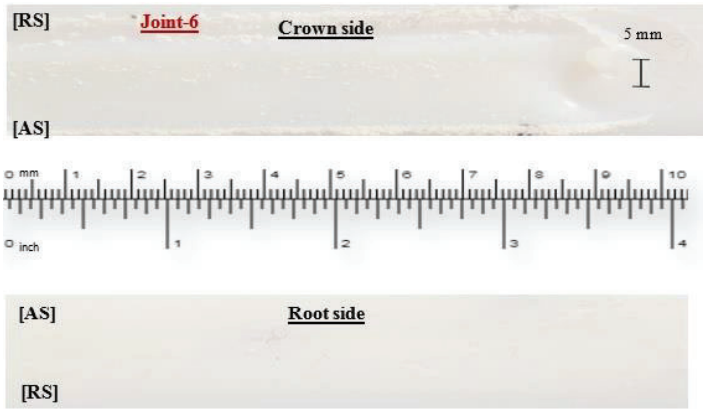

Fig. 10. Joint-6 material flow, surface finish, and surface defects

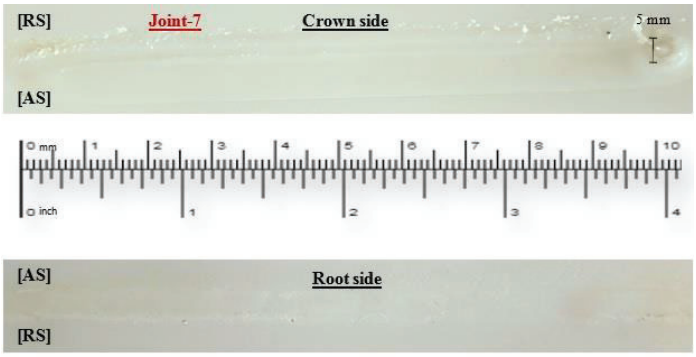

Fig. 11. Joint-7 material flow, surface finish, and surface defects

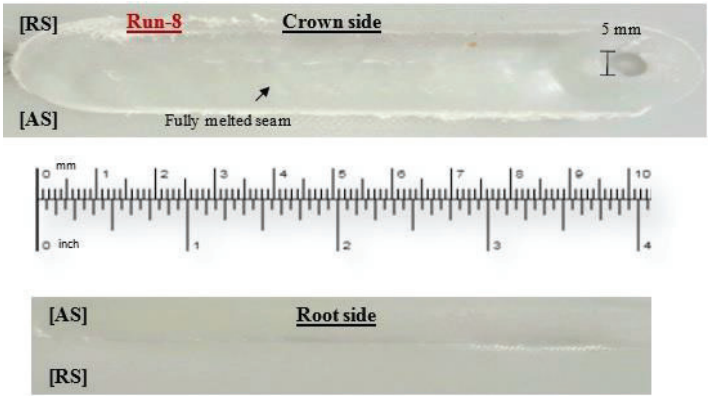

Fig. 12. Joint-8 material flow, surface finish, and surface defects

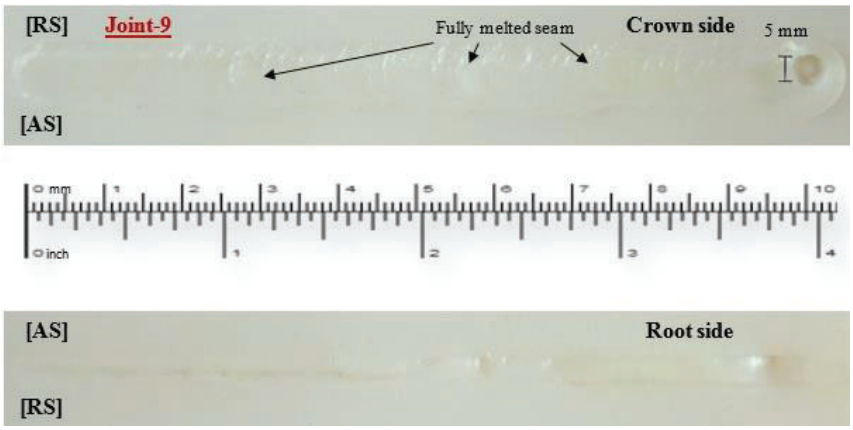

Fig. 13. Joint-9 material flow, surface finish, and surface defects

3.2 Tensile strength and percent elongation

The ultimate tensile strength and percent elongation before break of the samples are shown in Table-4. These values are reflective of the factors involved at its different combinations' values. Samples from joint-2 and joint-3 had very poor weld strength. The remaining joints resulted in good tensile strength and percent elongation values before break as compared to its base strength. However, the tensile strength values of samples from joint-4 were low but their percent-elongation-before-break value was good which means that its bond was not brittle like joint-2 and joint-3. While Joint-5, Joint-7, and Join-9 had very good tensile strength values almost identical to the strength value of the base material. However, their percent-elongation-before-break values are good compared to other joints, but they are poor compared to the value of the base material.

3.3 The fracture zone, nature, and profile of Joints' samples on tensile testing

A combined view of all specimens is shown in Figure 14. Most specimens resulted in ductile fracture. The fracture profile and zone are different for each specimen depending on the processing parameters.

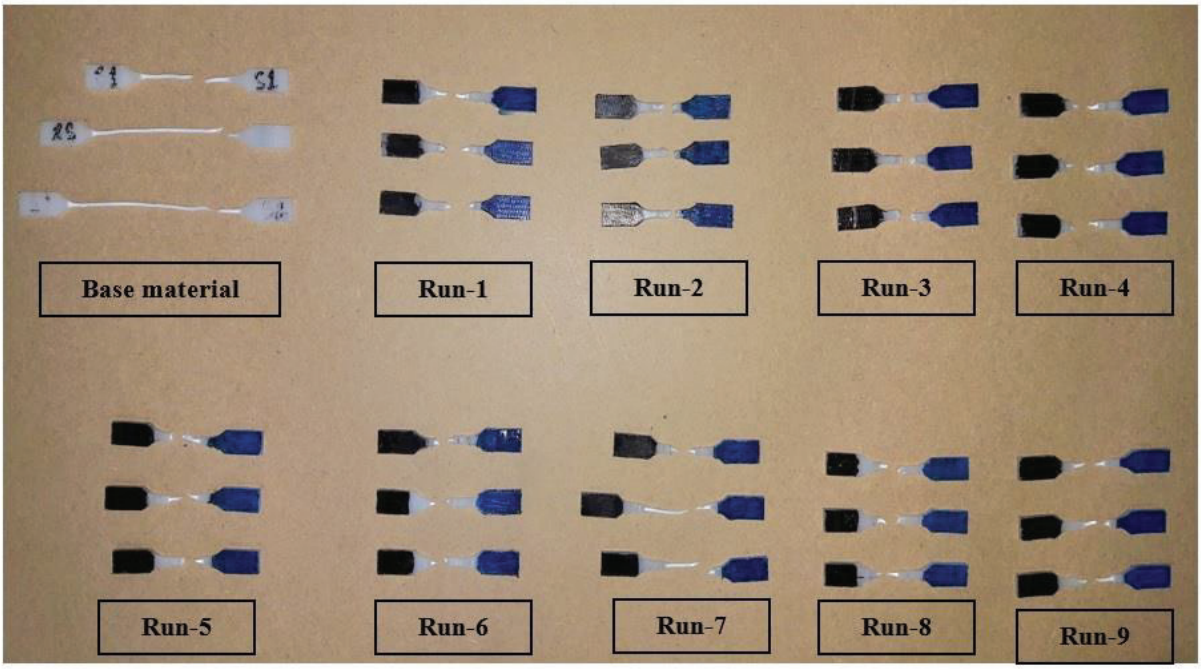

Fig. 14: Sample joint specimens after tensile tests

3.4 Taguchi analysis of UTS of joint samples

Based on the calculated SN ratios and Means of main effects, the highest value came for temperature at its highest level, the next highest value for traversing speed at its lowest level, and the least for rotational speed at its lowest speed value. The delta values given in Table 5 that denote the significance of each parameter. Based on the delta values, the ranking or order of significance is given to each processing parameter. The responses of each main effect are also shown in Fig. 15 & Fig.16. The Larger-is-better approach from equation-(1) was used for calculating the SN ratios because we wanted to maximize our response – the UTS of the joint.

$$SN_L = -10\log\left(\frac{1}{n}\sum_{i=1}^{n}\frac{1}{{y_i}^2}\right) \qquad Eq.1$$

Table 5: Main effects table of UTS using Signal to Noise Ratios [Larger is Better]

Level	Temperature(°C)	Rotational Speed(rpm)	Traversing Speed (mm/min)
1	21.82	25.26	25.82
2	25.19	24.72	23.72
3	26.60	23.62	24.05
Delta	4.78	1.63	2.10
Rank	**1**	**3**	**2**

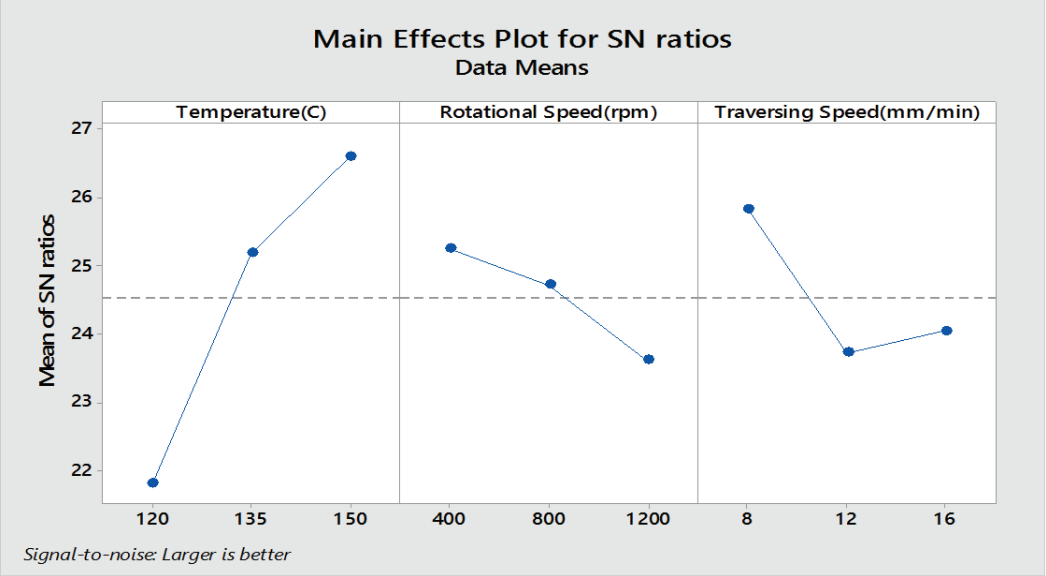

Fig. 15: Main effects plot of UTS using SN ratios

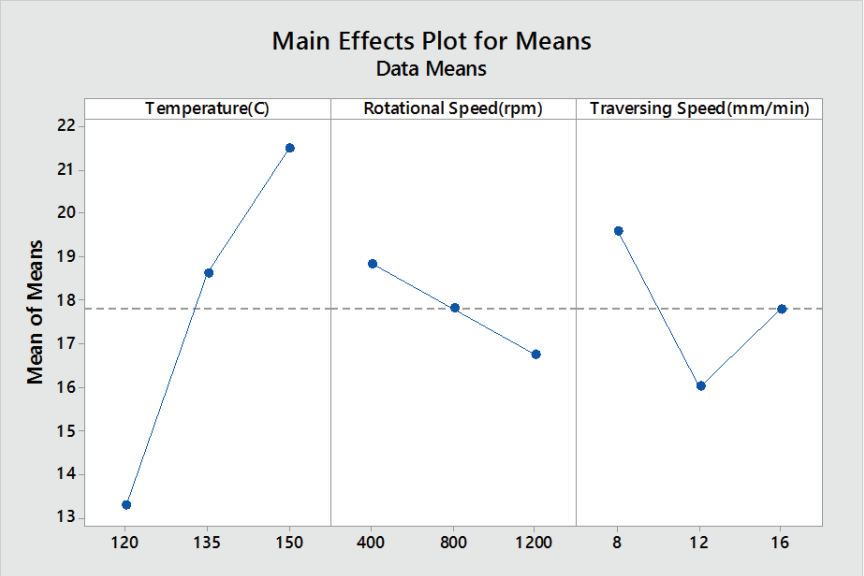

Fig. 16: Main effects plot of UTS using Means

3.5 Taguchi Analysis of Percent-Elongation-at-Break of joint samples

The Percent-Elongation-at-Break (%-EB) is also an important property of HDPE. SN ratios and Main Effects were used to identify the mutual contribution of each processing parameter as given in Tables 6 and Figures 17 & 18. The SN ratios and Means of main Effects show that temperature at its highest level has the most contribution towards %-EB followed by tool rotational speed and then tool traversing speed at their lowest levels. The larger-is-better equation approach form Equation (1) was again used as we wanted to maximize the response value i.e., %-EB.

Table 6: Main effects table of %-EB using Signal to Noise Ratios [Larger is Better]

Level	Temperature(°C)	Rotational Speed(rpm)	Traversing Speed(mm/min)
1	29.75	42.04	39.72
2	40.43	35.55	36.38
3	42.82	35.41	36.90
Delta	13.07	6.62	3.34

Rank	1	2	3

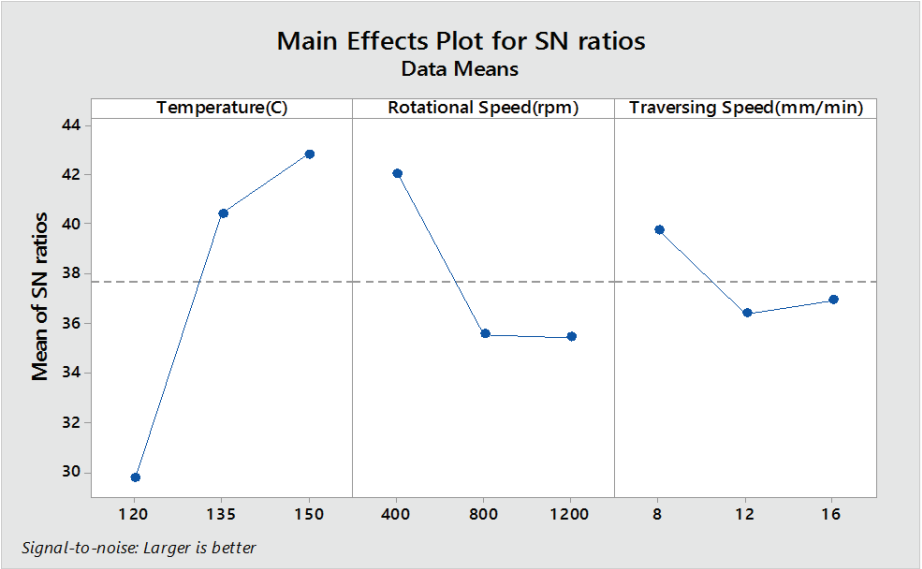

Fig. 17: Main effects plot of %-EB using SN ratios

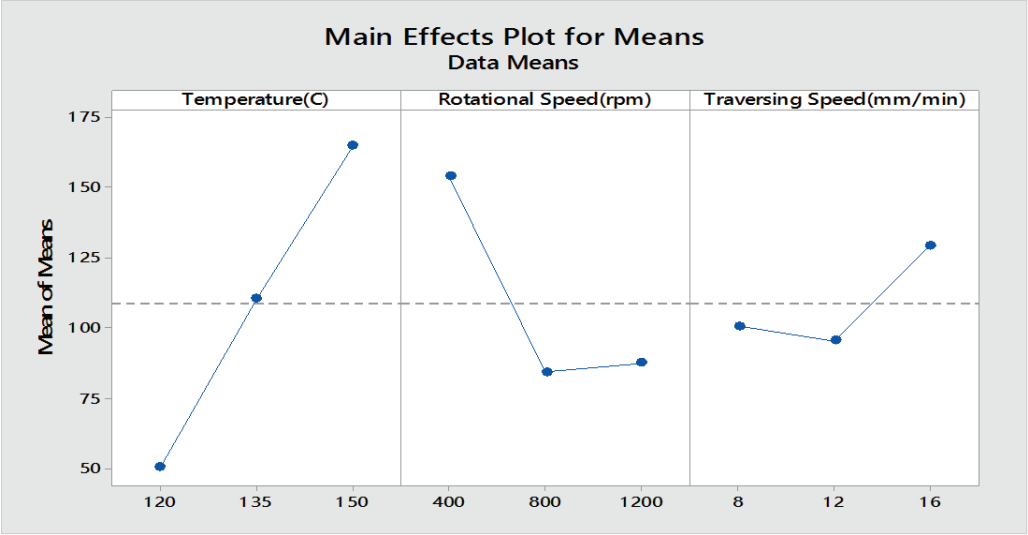

Fig. 18: Main effects plot of %-EB using Means

3.6 Confirmation experiment at optimum setting

Taguchi analysis also makes prediction based on the optimum settings of input factors. From the analysis of UTS as well as Percent-elongation-at-Break, the best setting is Temperature at its highest level, Rotational Speed at its lowest, and Traversing Speed also at its lowest speed. Using

Minitab®, the prediction setting at optimum parameters combination (Table 7) was taken and the predicted value for UTS came to be 24.2899 MPa as shown in Table 8.

Table 7: Prediction Settings

Temperature(C)	Rotational Speed(rpm)	Traversing Speed(mm/min)
150	400	8

Table 8: Prediction value

S/N Ratio	Mean
28.6066	**24.2899**

Hence an experiment was performed at the optimum condition of Temperature at its highest level (150 °C), Rotational Speed at its lowest level (400rpm), and Traversing Speed also at its lowest level (8 mm/min), the Actual value for UTS came to be **23.3 MPa**. The value is slightly less than the predicted value, but it is reasonable value as the predicted value can't exceed from the strength of the base material which has a strength of 23.5 MPa.

4. Discussions

The joints made are summarized in terms of their defects, defects' locations, fracture type, Percent-Elongation-at-Break, and the Ultimate Tensile Strength in Table 9 to show the overall behavior and quality of the joints made. Based on these results, the following sections will discuss the welding properties of the joint with reference to the processing parameters.

Table 9: Overall analysis of all joints

Joints	**Surface**	**Defects**	**Defects locations**	**Fracture Locations**	**Fracture Type**	%-EB	**UTS**
1	Crown	CD	AS	RS, C, AS	Ductile	20	117.6
	Root	CD	UD				

2	Crown	KB	UD	AS, AS, AS	Brittle	12	17.6
	Root	CD	UD				
3	Crown	KB	UD	C, C, C	Brittle	7.8	16.3
	Root	LOP	UD				
4	Crown	F, SLF	AS, RS	RS, RS, RS	Ductile	13.4	108.4
	Root	-	Start				
5	Crown	-	-	RS, C, AS	Ductile	22.6	136.6
	Root	-	-				
6	Crown	-	-	RS, RS, RS	Ductile	19.9	85.8
	Root	-	-				
7	Crown	SLF, F	RS	C, AS, AS	Ductile	23	234.7
	Root	-	-				
8	Crown	-	-	RS, RS, RS	Ductile	18.8	98.5
	Root	-	-				
9	Crown	B	UD	C, C, C	Ductile	22.6	160.4
	Root	CD	UD				

CD = Cavity defect, F = Flash, KB = Kissing Bond, LOP = Lack of Penetration defect, SLF = Surface Lack-of-Fill, B = bulging, AS = advancing side, RS = retreating side, C = center, UD = uniformly distributed.

4.1. Role of input parameters on mechanical properties

For UTS, it was found that the most significant factor is temperature followed by tool traversing speed and then tool rotational speed. Temperature at its highest level while tool traversing and rotational speeds at their lowest levels are needed to guarantee higher SN ratios and Means values for UTS (Table 5). Temperature increase has a positive effect while increasing it from the lowest to the highest level. This increase is almost linearly proportional when moving from low-level to mid-level and then from mid-level to high-level for both SN ratios and Means values (Fig 16). Tool rotational speeds also show a linearly proportional decrease in the SN ratios and Means values while moving from the lowest level to the mid-level of tool rpm, and then moving to the high level. For traversing speed, moving from the lowest level to the mid-level results in a steep decrease in both SN ratios and Means values while moving further from the mid-level to the high-level results in a slight upward increase in the ratio for SN ratio while a more pronounced increase in the Mean values. This means that for each factor there is an optimum level setting. And the overall idea from both SN ratios and Mean values is that temperature at its highest level while traversing and rotational speeds at their lowest levels guarantee best possible tensile strengths for the joints.

While in case of %-EB, the most significant factor is also temperature but followed by tool rotational speed and then tool traversing speed. Temperature needs to be at its high level for both SN ratios and Means values while tool rotational and traversing speeds need to be at their lowest levels for SN ratio but for traversing speed rotational speeds needs to be its lowest level while traversing speed at its high level (Table 6 and Figure 18). Moving up the levels of temperature increases both SN ratios and Means values at linear fashion. While moving up the levels of tool rotational speed have first a steep decreasing effect and then a slight decreasing effect for SN ratios or slightly increasing effect for Means values when moved from low level to mid-level and then from mid-level to the high level. For SN ratio, traversing speed at its low-level has the most effect on %-EB while for Means values, traversing speed at its high-level has the most effect on %-EB.

Hence for both UTS and %-EB, the order of significance can be taken as temperature being the most important factor of all, followed by the tool rotational speed, and then tool traversing speed. The best joint made in terms of both UTS and %-EB is through run-7 which give us the highest possible strength and strain values.

4.2. Role of input parameters in defects formation

Temperature near the melting range of HDPE is necessary for proper consolidation. Below the melting range and when the heat flow time was comparatively less, kissing bonds defects arises while above the melting range and with the heat flow time relatively high, material flash happens. Bulging of the weld also occurs at high melting range but the reason for that was the lower plunging power of the shoulder because of the high temperature. Surface Lack-of-Fill defects arise where the rotational speeds are low, and the traversing speeds are high. Material flash also occurs in conjunction with surface Lack-of-Fill defects. Cavity defects occur when either rotational speed is low or traversing speed is high or both settings at the same time. The reason for cavities is the lack of plunging force at high values of temperature. Weld sinks arise as a result the void left when the tool is retracted back from the seam material. Lack-of-penetration defect occurs because of the tool not plunging to full depth while the temperature is its low-level value.

In addition to these, some defects can also be attributed to the tool design parameters and motion. Because of the flat design of shoulder and rotational motion, particles from the seam region were flown away and hence resulted in different surface defects.

4.3. Welding parameters

The welding parameters used in this study were found to have a considerable effect on the weld quality. Temperature was found to be the most significant factor both in terms of UTS and %-EB. The SN ratios and Means values indicates that temperature needs to be at its highest level and rotational and traversing speeds are needed to be at their lowest levels in order to obtain the best response both in terms of UTS and %-EB of joints. Although Pirizadeh et al. [22] concluded in their work that rotational speeds are needed to be its highest level and traversing speed at the medium level in contrast to the current work but the reason is that they didn't consider external heat supply in their work. Vijendra and Sharma [10] used external heat only up to 55 °C and to raise the temperature to the required level they applied high rotational speed of 2000 rpm. The result was that they got high quality weld in terms of joint strength but slightly poor quality in terms of %-EB as the maximum reported value is only up to 23.55% while the %-EB reported in this work is up to 34%. The reason for this can be explained by the breaking of monomer chains

due to high rotational speeds. The processing parameters used in this study are much closer to the parameters used for FSW of Nylon-6 by Mustafapour and Asad Taghizad [36] who reported joint strength efficiency of 98%, which is the same value obtained in this work.

4.3. Joint efficiency

The joint efficiency obtained in this work is given in terms of UTS (Eq. 2), %-EB (Eq. 3), and for both UTS and %-EB combined (Eq. 4).

$$Joint\ Efficiency_{UTS} = \left(\frac{UTS_{best\ joint}}{UTS_{base\ material}}\right) * 100 \quad \text{(Eq. 2)}$$

$$= \left(\frac{23.04}{23.53}\right) \times 100\%$$

$$= 97.9\%$$

$$\cong 98\%$$

Also,

$$Joint\ Efficiency_{\%EB} = \left(\frac{\%EB_{best\ joint}}{\%EB_{base\ material}}\right) * 100 \quad \text{(Eq. 3)}$$

$$= \left(\frac{234.8}{692.7}\right) \times 100\%$$

$$= 33.9\%$$

$$\cong 34\%$$

And,

$$JE_{Combined} = [0.5(JE_{UTS}) + 0.5(JE_{\%EB})] \quad \text{(Eq. 4)}$$

Whereas JE = Joint Efficiency.

$$= [0.5(97.9\%) + 0.5(33.9\%)]$$

$$= 65.9\%$$

$$\cong 66\%$$

The joint efficiency in terms of UTS came to be 98%. In terms of %-EB, the efficiency came to be only 34%. While for the combined effect of UTS and %-EB, the efficiency came to be 66%. The joint efficiency closer to 100% in terms of UTS is also reported for nylon-6 and HDPE in research works in which heat is externally supplied to the weld seam [36],[10]. UTS alone isn't indicative of weld quality which is frequently used as the target to achieve. The reason for this is that having a best strength value doesn't mean that the joint is welded in the best way possible as there are other inherent properties which are affected adversely in the same process. Hence in this work, we took %-EB as another desired property to achieve in conjunction with UTS to express the true joint efficiency.

4.4. Welding defects

Most joints made through heat assisted FSW were free of defects and ensured good joint quality and strength. The few defects which affected the weld quality were Flash, Outpouring, Surface Lack-of-Fill, and Kissing bonds. Flash and Outpouring resulting from overheating of seam material which caused unsuccessful welds while Kissing bonds resulting from under-heating of seam material which resulted in poor weld consolidation. The Surface Lack-of-Fill defects arose in joints where rotational speed was low and traversing speed was high which caused reduced material rotation at the retreating side. This effect was explained by Zhang and Chen in their work of finite element simulation of FSW process [37]. Saeedy and Givi [14] concluded in the microstructural study of the joints that micro cracks and voids caused the reduction of strength in FSW joints. Kissing bonds in this work resulted in similar micro cracks and voids and hence the joints made had lower strength values. Other defects like surface Lack-of-Fill defects and voids resulted in stress concentration in their regions which greatly reduced the %-EB of joints.

5. Conclusions:

The conclusions that can be drawn from the results and discussion sections are given as follows.

- FSW of thermoplastics materials using a heated assisted tool can be performed on CNC milling machine and can be automated.

- Using heat-assisted tool, welding can be done efficiently with low levels of rotational and traversing speeds.
- Using the developed heat-assisted tool weld efficiency of 98% in terms of UTS was achieved, hence weld strength equal or closer to the base material is possible using a proper combination of welding parameters.
- The maximum weld efficiency achieved for %-EB was only 34%.
- The combined weld efficiency in terms of both UTS and %-EB was only 66% hence suggesting that alone weld strength efficiency, which is 98% of the base material, doesn't fully describe the weld quality.
- Surface Lack-of-fill defects arose at the retreating side of joints because of low rotational speed and high traversing speeds which caused uneven mixing of seam material. Cavity defects arose where temperature was at low-level caused by poor mixing of seam material or where it was at high level and caused by the poor plunging force because of the outpouring of seam material under the shoulder of tool. Flash and outpouring occurred at high levels of temperature because of over-heating.
- The best weld quality in terms of both UTS and %-EB occurred in Run-7 at high levels of temperature and traversing speeds and low level of rotational speed.
- The SN ratios and Mean values of main effects show that temperature is the most important input parameter followed by rotational and traversing speeds for both UTS and %-EB.

6. Funding Information

This research did not receive any specific grant from funding agencies in the public, commercial, or not-for-profit sectors.

7. Conflict of Interest

The authors declare that they have no conflict of interest.

7. References

[1] R. S. Mishra and Z. Y. Ma, "Friction stir welding and processing," *Mater. Sci. Eng. R Reports*, vol. 50, no. 1–2, pp. 1–78, 2005, doi: 10.1016/j.mser.2005.07.001.

[2] A. S. Vasava, H. B. Patel, B. Desai, and V. Naik, "Review paper on friction stir welding," *Int. Res. J. Eng. Technol.*, vol. 3, no. 12, pp. 505–510, 2016.

[3] Kalpana Mistry, "Plastics welding," *Assem. Autom.*, vol. 17, no. 3, pp. 196–200, 2015.

[4] S. Strand, "Joining plastics - can friction stir welding compete?," in *Electrical Insulation Conference and Electrical Manufacturing and Coil Winding Technology Conference*, 2003, pp. 321–326. doi: 10.1109/EICEMC.2003.1247904.

[5] F. Simoes and D. M. Rodrigues, "Material flow and thermo-mechanical conditions during Friction Stir Welding of polymers: Literature review, experimental results and empirical analysis," *Mater. Des.*, vol. 59, pp. 344–351, 2014, doi: 10.1016/j.matdes.2013.12.038.

[6] M. K. Bilici, A. İ. Yükler, and M. Kurtulmuş, "The optimization of welding parameters for friction stir spot welding of high density polyethylene sheets," *Mater. Des.*, vol. 32, no. 7, pp. 4074–4079, 2011, doi: 10.1016/j.matdes.2011.03.014.

[7] Y. Bozkurt, "The optimization of friction stir welding process parameters to achieve maximum tensile strength in polyethylene sheets," *Mater. Des.*, vol. 35, pp. 440–445, 2012, doi: 10.1016/j.matdes.2011.09.008.

[8] S. Hoseinlaghab, S. S. Mirjavadi, N. Sadeghian, I. Jalili, M. Azarbarmas, and M. K. Besharati Givi, "Influences of welding parameters on the quality and creep properties of friction stir welded polyethylene plates," *Mater. Des.*, vol. 67, pp. 369–378, 2015, doi: 10.1016/j.matdes.2014.11.039.

[9] Amir Mostafapour & Ehsan Azarsa, "A study on the role of processing parameters in joining polyethylene sheets via heat assisted friction stir welding: Investigating microstructure, tensile and flexural properties," *Int. J. Phys. Sci.*, vol. 7, no. 4, pp. 647–654, 2012, doi: 10.5897/IJPS11.1653.

[10] B. Vijendra and A. Sharma, "Induction heated tool assisted friction-stir welding (i-FSW):

A novel hybrid process for joining of thermoplastics," *J. Manuf. Process.*, vol. 20, pp. 234–244, 2015, doi: 10.1016/j.jmapro.2015.07.005.

[11] V. Jaiganesh, B. Maruthu, and E. Gopinath, "Optimization of process parameters on friction stir welding of high density polypropylene plate," *Procedia Eng.*, vol. 97, pp. 1957–1965, 2014, doi: 10.1016/j.proeng.2014.12.350.

[12] M. A. Rezgui, A. Trabelsi, M. Ayadi, and K. Hamrouni, "Optimization of Friction Stir Welding Process of High Density Polyethylene Optimization of Friction Stir Welding Process of," no. FEBRUARY, 2011.

[13] E. A. Squeo, G. Bruno, A. Guglielmotti, and F. Quadrini, "Friction stir welding of polyethylene sheets," *Frict. stir Weld. Polyethyl. sheets*, pp. 241–146, 2009.

[14] S. Saeedy and M. K. Besharati Givi, "Investigation of the effects of critical process parameters of friction stir welding of polyethylene," *Proc. Inst. Mech. Eng. Part B J. Eng. Manuf.*, vol. 225, p. 09544054JEM1989, 2010, doi: 10.1038/2201159a0.

[15] A. Arici and T. Sinmaz, "Effects of double passes of the tool on friction stir welding of polyethylene," *J. Mater. Sci.*, vol. 40, no. 12, pp. 3313–3316, 2005, doi: 10.1007/s10853-005-2709-x.

[16] M. Aydin, "Effects of Welding Parameters and Pre-Heating on the Friction Stir Welding of UHMW-Polyethylene," *Polym. Plast. Technol. Eng.*, vol. 49, no. 6, pp. 595–601, 2010, doi: 10.1080/03602551003664503.

[17] M. K. Bilici, "Application of Taguchi approach to optimize friction stir spot welding parameters of polypropylene," *Mater. Des.*, vol. 35, pp. 113–119, 2012, doi: 10.1016/j.matdes.2011.08.033.

[18] K. Panneerselvam and K. Lenin, "Investigation on Effect of Tool Forces and Joint Defects During FSW of Polypropylene Plate," *Procedia Eng.*, vol. 38, pp. 3927–3940, 2012, doi: 10.1016/j.proeng.2012.06.450.

[19] Z. Kiss and T. Czigány, "Applicability of friction stir welding in polymeric materials," *Period. Polytech.*, vol. 51, no. 1, pp. 15–18, 2007, doi: 10.3311/pp.me.2007-1.02.

[20] G. H. Payganeh, N. B. M. Arab, Y. D. Asl, F. a. Ghasemi, and M. S. Boroujeni, “Effects of friction stir welding process parameters on appearance and strength of polypropylene composite welds,” *Int. J. Phys. Sci.*, vol. 6, no. 19, pp. 4595–4601, 2011, doi: 10.5897/IJPS11.866.

[21] A. Bagheri, T. Azdast, and A. Doniavi, “An experimental study on mechanical properties of friction stir welded ABS sheets,” *Mater. Des.*, vol. 43, pp. 402–409, 2013, doi: 10.1016/j.matdes.2012.06.059.

[22] M. Pirizadeh, T. Azdast, S. Rash Ahmadi, S. Mamaghani Shishavan, and A. Bagheri, “Friction stir welding of thermoplastics using a newly designed tool,” *Mater. Des.*, vol. 54, pp. 342–347, 2014, doi: 10.1016/j.matdes.2013.08.053.

[23] N. Mendes, A. Loureiro, C. Martins, P. Neto, and J. N. Pires, “Effect of friction stir welding parameters on morphology and strength of acrylonitrile butadiene styrene plate welds,” *Mater. Des.*, vol. 58, pp. 457–464, 2014, doi: 10.1016/j.matdes.2014.02.036.

[24] N. Sadeghian and M. K. Besharati Givi, “Experimental optimization of the mechanical properties of friction stir welded Acrylonitrile Butadiene Styrene sheets,” *Mater. Des.*, vol. 67, pp. 145–153, 2015, doi: 10.1016/j.matdes.2014.11.032.

[25] K. Panneerselvam and K. Lenin, “Joining of Nylon 6 plate by friction stir welding process using threaded pin profile,” *Mater. Des.*, vol. 53, pp. 302–307, 2014, doi: 10.1016/j.matdes.2013.07.017.

[26] E. Azarsa and A. Mostafapour, “Experimental investigation on flexural behavior of friction stir welded high density polyethylene sheets,” *J. Manuf. Process.*, vol. 16, no. 1, pp. 149–155, 2014, doi: 10.1016/j.jmapro.2013.12.003.

[27] M. A. Rezgui, M. Ayadi, A. Cherouat, K. Hamrouni, A. Zghal, and S. Bejaoui, “Application of Taguchi approach to optimize friction stir spot welding parameters of polypropylene,” *Mater. Des.*, vol. 35, pp. 113–119, 2010, doi: 10.1016/j.matdes.2011.08.033.

[28] S. H. Dashatan, T. Azdast, S. R. Ahmadi, and A. Bagheri, “Friction stir spot welding of dissimilar polymethyl methacrylate and acrylonitrile butadiene styrene sheets,” *Mater.*

Des., vol. 45, pp. 135–141, 2013, doi: 10.1016/j.matdes.2012.08.071.

[29] N. Mendes, A. Loureiro, C. Martins, P. Neto, and J. N. Pires, "Morphology and strength of acrylonitrile butadiene styrene welds performed by robotic friction stir welding," *Mater. Des.*, vol. 64, pp. 81–90, 2014, doi: 10.1016/j.matdes.2014.07.047.

[30] S. Eslami, T. Ramos, P. J. Tavares, and P. M. G. P. Moreira, "Effect of Friction Stir Welding Parameters with Newly Developed Tool for Lap Joint of Dissimilar Polymers," *Procedia Eng.*, vol. 114, pp. 199–207, 2015, doi: 10.1016/j.proeng.2015.08.059.

[31] S. Eslami, T. Ramos, P. J. Tavares, and P. M. G. P. Moreira, "Shoulder design developments for FSW lap joints of dissimilar polymers," *J. Manuf. Process.*, vol. 20, pp. 15–23, 2015, doi: 10.1016/j.jmapro.2015.09.013.

[32] A. Zafar, M. Awang, and S. R. Khan, "Friction Stir Welding of Polymers: An Overview," 2017. doi: 10.1007/978-981-10-4232-4.

[33] S. Eslami, P. J. Tavares, and P. M. G. P. Moreira, "Friction stir welding tooling for polymers: review and prospects," *Int. J. Adv. Manuf. Technol.*, vol. 89, no. 5–8, pp. 1677–1690, 2017, doi: 10.1007/s00170-016-9205-0.

[34] A. Scialpi, M. Troughton, S. Andrews, and L. A. C. De Filippis, "Viblade ^{TM} : friction stir welding for plastics," vol. 7116, no. December, 2017, doi: 10.1080/09507110902843271.

[35] Su, H., Wu, C.S., Pittner, A., Rethmeier, M., 2013. Simultaneous measurement of tooltorque, traverse force and axial force in friction stir welding. *J. Manuf. Processes* 15,495–500.

[36] A. Mostafapour and F. Taghizad Asad, "Investigations on joining of Nylon 6 plates via novel method of heat assisted friction stir welding to find the optimum process parameters," *Sci. Technol. Weld. Join.*, vol. 21, no. 8, pp. 660–669, 2016, doi: 10.1080/13621718.2016.1169669.

[37] H. W. Zhang, Z. Zhang, and J. T. Chen, "The finite element simulation of the friction stir welding process," vol. 403, pp. 340–348, 2005, doi: 10.1016/j.msea.2005.05.052.